Radargrammetry and SAR interferometry for DEM generation: validation and data fusion

Michele Crosetto [(1)], Fernando Pérez Aragues [(2)]

(1) DIIAR - Sez. Rilevamento, Politecnico di Milano
P. Leonardo Da Vinci 32, 20133 Milan, Italy
Tel: ++39-02-2399-6503 E-mail: miche@ipmtf4.topo.polimi.it

(2) ICC - Institut Cartografic de Catalunya
Parc de Montjuic, E-08038 Barcelona, Spain
Tel: ++34-93-425-2900 E-mail: fernandop@icc.es

ABSTRACT

This paper describes the generation of digital elevation models (DEMs) with the radargrammetric and interferometric techniques. In the first part, the main characteristics of the two procedures implemented at ICC and Polytechnic of Milan are presented. Particular emphasis is given to the geometric aspects of the two procedures, which allow achieving an accurate geo-location of the generated DEMs. In the second part, the results obtained processing ERS-1 and Radarsat images are analysed. The generated DEMs were validated over a test area using a suited reference DEM. In this way it was possible to compare the performances of the two procedures and to investigate their complementarity. In the last part of the paper, an example of interferometric and radargrammetric data fusion for the compensation of the atmospheric artefacts that affect the InSAR DEMs is presented.

1. INTRODUCTION

Since the advent of the first spaceborne systems, DEM generation has been mainly based on optical imagery and photogrammetric techniques. SAR images are recently gaining importance thanks both to the large availability of spaceborne SAR data and the development of different techniques to exploit them. Starting from SAR images, DEMs can be generated exploiting either the amplitude (radargrammetry or shape from shading techniques) or the phase of the radar signal (interferometric techniques). In this paper only radargrammetry and interferometry are considered.

Radargrammetry works with amplitude SAR images utilising the same approach that photogrammetry uses with optical images. This technique is usually employed with stereoscopic pairs acquired from the same side but with different incidence angles. Its importance has increased in the last years, especially since the launch in November 1995 of Radarsat, the first commercial system that allows acquiring SAR stereo pairs with a large range of incidence angles. Radargrammetry can be implemented using an interactive approach or an automated one. In the interactive one, based on analytical or digital photogrammetric systems adapted to SAR images, the operator must capture the data manually [1], [2]. In the second kind of approach, based on image correlation algorithms suited to extract pairs of homologous points (matching), the operator becomes a supervisor of an automatic (or semi-automatic) measurement process [3], [4]. In the following sections, only the automated approach is addressed.

Interferometric SAR (InSAR) is based on the processing of complex SAR images acquired from slightly different points of view. InSAR was proposed by Graham in 1974 and applied for the first time at JPL (Jet Propulsion Laboratories) in 1986 using airborne data [5]. Today, a large number of research groups are working on DEM generation with InSAR data coming from different airborne and spaceborne systems. The importance of InSAR is related to its high spatial resolution and good potential precision and to the highly automated DEM generation capabilities.

In the following sections, the main characteristics of the radargrammetric and InSAR procedures implemented at ICC and Polytechnic of Milan respectively are described. Particular emphasis is given to the geometric aspects of the two procedures.

2. A RADARGRAMMETRIC PROCEDURE

The radargrammetric procedure implemented at ICC allows generating DEMs in a fully automatic way. The entire process consists of three main stages:

- First, the accurate geometric correspondence between image space and object space must be established.
- Then, solving an inverse trisection problem we obtain the coordinates (X,Y,Z) of each terrain point whose image coordinates (col_1, lin_1) and (col_2, lin_2) are found via a correlation process.

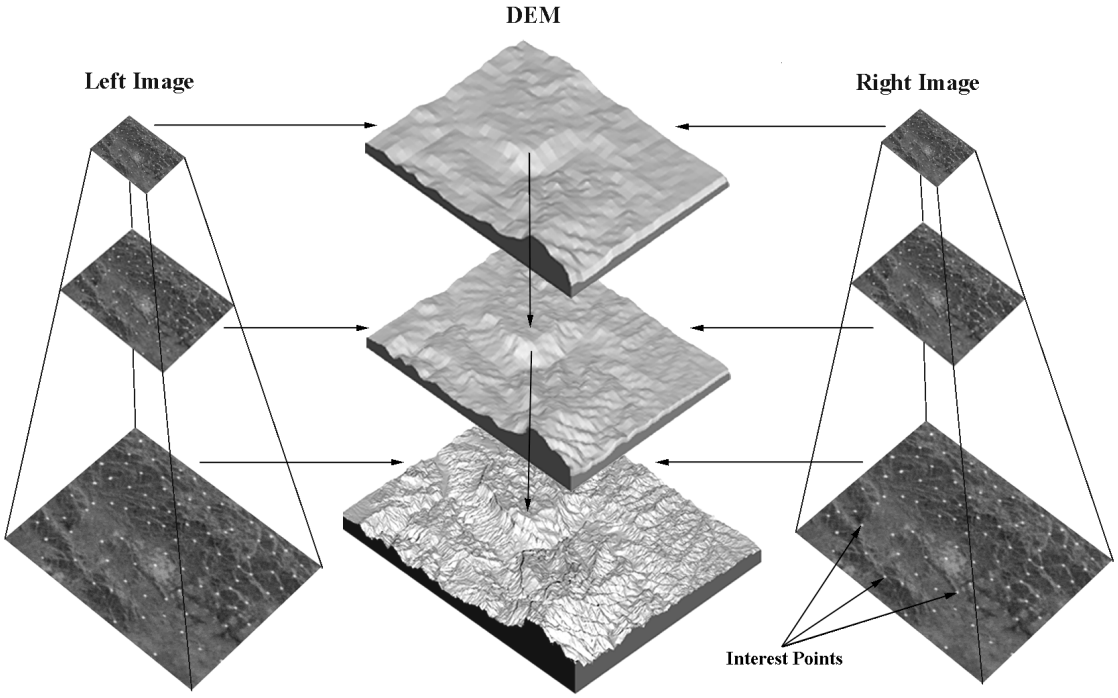

Fig. 1: Image pyramids and interest points

- The huge number of points obtained enter a finite-element adjustment where the whole DEM area is divided in tiles and continuity constraints between tiles are imposed. In this way we eliminate blunders and wrong matches and we get the final raster DEM (regular grid).

In order to establish the image to object space correspondence, a rigorous SAR image formation model (SIFM) must be defined. Furthermore, the model parameters, often known with inadequate accuracy, have to be refined through a calibration procedure based on the measurement of tie points and ground control points (GCPs). The SIFM and the calibration are described in detail in the following sections.

The image correlation algorithms suited to radargrammetry have to take into account the geometric peculiarities of SAR images. The correlation procedure employed at ICC, developed for optical stereo pairs (SPOT) and then adapted to SAR images, uses an area-based matching applied to a pyramid of images where some outstanding features have been found. Firstly, a pyramid of images is created starting from the original images, where the pixel size on each step doubles the size of the proceeding one. Then, the Förstner algorithm [6] is applied to each image level to obtain a set of points that are good candidates for image correlation (interest points, see Fig. 1). Each point is matched with its homologous on the other image shifting up and down the terrain height until optimum correlation is obtained. A subsequent adjustment on the correlation value permits further refinement in this level. The upper the pyramid level, the coarser the obtained DEM grid and the larger the height shifts. Hence, descending through the pyramid, we obtain a finer and finer DEM ensuring at the same time continuity and stability to the process.

2.1. SAR Image Formation Model

An important step in the implementation of a radargrammetric process is the definition of a rigorous SIFM. The one adopted at ICC is based on the two basic SAR mapping equations, namely the range and the Doppler equations:

$$R_S = \left|(\vec{P} - \vec{S})\right| = SP \qquad (1)$$

$$f_D = -\frac{2 \cdot \overrightarrow{SP} \cdot \vec{V}_S}{\lambda \cdot SP} \qquad (2)$$

where $\vec{P} = (X_P, Y_P, Z_P)$ is the location of the target point on the ground, $\vec{S} = (X_S, Y_S, Z_S)$ is the satellite position, $\vec{V}_S$ is the satellite velocity vector, R_S is the slant range distance, f_D is the Doppler centroid frequency and λ is the radar wavelength. The SIFM includes different groups of parameters: orbital parameters, sensor parameters and SAR processing parameters. Working

usually over relatively small areas, we use a polynomial model for orbit description:

$$\begin{aligned} X_S &= a_0 + a_1 \cdot t_R + a_2 \cdot t_R^2 + a_3 \cdot t_R^3 \\ Y_S &= b_0 + b_1 \cdot t_R + b_2 \cdot t_R^2 + b_3 \cdot t_R^3 \\ Z_S &= c_0 + c_1 \cdot t_R + c_2 \cdot t_R^2 + c_3 \cdot t_R^3 \end{aligned} \quad (3)$$

where $t_R = t - t_0$, t is the time parameter, t_0 is the acquisition time of the first image line and (X_S,Y_S,Z_S) are the satellite coordinates. The coefficients of the polynomials (a_i ,b_i ,c_i) are estimated by least squares (LS) adjustment using few orbital points whose coordinates are available in the image header or in the precise orbit products which can be purchased through the image providers. For a given target point, the acquisition time t is related to the azimuth coordinate (lin) of the SAR image through:

$$t = t_0 + \Delta t \cdot (lin - 1) \quad (4)$$

where Δt is related to the pixel size in azimuth direction. The slant range distance R_S is related to the slant range coordinate (col_S) through:

$$R_S = R_{S0} + \Delta R \cdot (col_S - 1) \quad (5)$$

where R_{SO} is the near slant range and ΔR is the pixel size in range. Working with images given in ground range geometry, we have to include in the SIFM the equation which connects slant range (col_S) and ground range (col_G) coordinates:

$$col_G = g_0 + g_1 \cdot col_S + g_2 \cdot col_S^2 + g_3 \cdot col_S^3 \quad (6)$$

This equation is omitted when working with slant range images.

2.2. Model Parameter Refinement

Some of the model parameters are known with inadequate accuracy. In order to obtain an accurate geolocation, these parameters have to be refined by a LS calibration based on the measure of GCPs and tie points. Working with a stereo pair of SAR images, these are the model parameters treated as unknowns in the calibration: the near slant range R_{SO}, the acquisition time of the first image line t_0, the pixel size in azimuth direction Δt and the coefficients of the orbit polynomials. The parameters R_{SO}, t_0 and Δt are considered constant within a SAR scene. The polynomial coefficients are refined in case the given orbits are not accurate enough (e.g. when only preliminary orbits are available). In this case a suited weighting of the coefficients has to be performed.

It is important to underline that the calibration can be used to simultaneously refine the parameters of different stereo SAR image pairs. The joint calibration of multiple pairs can be accomplished measuring both GCPs and tie points. The great advantage of such a calibration is the determination of a unique set of geometrically consistent SIFMs suited to obtain an accurate geolocation of the generated DEMs (i.e. a good DEM merging). The identification and measurement of GCPs on the images is performed manually. For tie points to be collected in same-side image pairs an automatic measurement is employed, while a manual one is used in opposite-side image pairs. Once GCPs and tie points are measured, the joint calibration allows to simultaneously estimating all SIFM parameters of the given SAR image set (block adjustment). The adjustment is carried out with a LS iterative procedure. For a good convergence, a suited weighting of the observations is needed. The weight selection, the initial parameter values and the quality of GCPs and tie points determine the convergence rate of the process.

3. AN InSAR PROCEDURE

The InSAR procedure implemented at DIIAR-Polytechnic of Milan includes several processing stages namely the image registration, the interferogram calculation and filtering, the image coherence calculation, the phase unwrapping, the generation of the irregular grid of 3D points and the interpolation of the final regular grid. The first three processing stages are based on the ISAR-Interferogram Generator software (distributed, free of charges, by ESA-ESRIN), an effective tool to obtain good filtered interferograms and the related coherence images [7]. The phase unwrapping is based on the "branch cuts" approach [8]. The most original parts of the procedure are the rigorous model for the conversion from interferometric phases to terrain heights and the calibration of the InSAR geometry based on GCPs. Both the InSAR model and the calibration are described in next section. An important aspect of InSAR is the influence of atmospheric distortions on the quality of the generated DEMs. The characteristics of such distortions and a strategy to compensate them using low-resolution auxiliary data are described in section 3.2.

3.1 InSAR Model and Geometry Refinement

For the transformation from interferometric phases to terrain heights we adopt a rigorous model that connects the image space (azimuth, slant range and interferometric phase) to the object space (usually a geocentric Cartesian system). The procedure works pixelwise: for each pixel of the interferogram, we derive the object space coordinates of the pixel footprint $P(X,Y,Z)$ using the slant range (1), the Doppler (2) and the interferometric equations.

For each interferogram pixel we derive the acquisition time t (4) and the slant range distance R_S (5). Then, we

calculate positions (3) and velocities of the master *M* and slave *S* satellites. *M*, *S* and the pixel footprint *P* are assumed to lie in the same plane (the Doppler centroid plane or antenna mid-plane that goes through *M*). We look for the position *S* of the slave satellite that fulfils the following equation:

$$\overrightarrow{MS} \cdot \vec{V}_M = -\lambda \cdot MS \cdot \frac{f_D}{2} \qquad (7)$$

where $\overrightarrow{\mathrm{MS}}$ is the baseline vector, $\vec{\mathrm{V}}_\mathrm{M}$ is the master velocity vector and *MS* is the slave-to-master distance (baseline length). The object space coordinates of the pixel footprint *P*(*X*,*Y*,*Z*) are estimated using the two basic SAR mapping equations (1) and (2), and the interferometric equation:

$$SP = MP + D_{IC} + \frac{\Phi_U \cdot \lambda}{4 \cdot \pi} \qquad (8)$$

where *MP* and *SP* are the master and slave slant range distances, Φ_U is the unwrapped phase, and D_{IC} is the interferometric constant. Repeating the procedure for all the pixels of the unwrapped interferogram, an irregular grid of 3D points is generated. Point coordinates refer to the geocentric Cartesian system used for the orbits, thus a transformation to a cartographic system and to orthometric heights is usually performed. Finally does the resampling to get the final regular geocoded grid follow.

As described above for the radargrammetric procedure, some of the model parameters used in the InSAR DEM generation have to be refined by a LS calibration. These are the model parameters treated as unknowns in the calibration: the near slant range R_{SO}, the pixel size in range direction ΔR, the acquisition time of the first image line t_0, the pixel size in azimuth direction Δt, the Doppler centroid frequency f_D and the interferometric constant D_{IC}. The parameters R_{SO}, ΔR, t_0 and Δt are considered constant within a SAR scene. For the Doppler centroid frequency a bilinear variation over the SAR image is considered:

$$f_D = f_{D0} + f_{D1} \cdot lin + f_{D2} \cdot col + f_{D3} \cdot lin \cdot col \qquad (9)$$

where f_{D0}, f_{D1}, f_{D2}, and f_{D3} have to be estimated in the adjustment. The parametrization of $\mathrm{D_{IC}}$ is of the form:

$$D_{IC} = d_0 + d_1 \cdot lin + d_2 \cdot col + d_3 \cdot lin \cdot col \qquad (10)$$

where the coefficients d_i have to be estimated in the adjustment. This kind of parametrization allows taking into account the phase unwrapping integration constant, the effect of orbit errors on the interferometric distance (*SP*–*MP*), and the linear atmospheric effects on the interferometric phase. There is a single unwrapping constant for the entire scene only if one integration zone is created during the unwrapping. Otherwise, for each zone a different constant has to be estimated.

The model parameters are refined by LS adjustment using GCPs. Recovering the GCPs necessary for the calibration of each pair is often hard and time consuming. The procedure we implemented allows fusing height data coming from multiple InSAR pairs (e.g. ascending and descending pairs). A joint calibration of all pairs, based on the measure of tie points, can be performed. It allows obtaining an accurate geolocation of the generated DEMs with a reduced number of GCPs.

3.2 Atmospheric Artefacts and Data Fusion

In InSAR DEM generation, signal propagation in a medium with constant refractive index is assumed. Indeed, changes in the refractive index between two image acquisitions may happen, causing distortions in the interferometric phase. These changes are mainly due to variations of atmospheric relative humidity [9]. Atmospheric variability results in artefacts (e.g. depressions) interpreted as terrain relief. A single pair can not check the presence of such artefacts, and this represents a very important limit of the InSAR technique.

A reduction of atmospheric artefacts can be obtained combining the information coming from multiple interferograms. We propose a strategy based on the use of auxiliary height data. We assume to use low-resolution data (e.g. with a resolution 10 times lower the one of the InSAR DEMs). Firstly, the InSAR and auxiliary data are accurately geolocated with respect to the same reference system. The fusion procedure employs a multiresolution data analysis in the space domain. We adopt two resolution levels: the first one corresponds to the high frequency components of the terrain topography contained in the InSAR data and the second one corresponds to the low frequency components contained in the auxiliary data. The output DEM contains the high frequency components of the original InSAR DEM and the low frequency components (not affected by atmospheric effects) of the auxiliary data. The proposed procedure represents a deterministic approach to the atmospheric artefact compensation: the low spatial frequencies of the corrected DEM are only estimated with the auxiliary data. A more rigorous approach should estimate the low frequency components of the DEM taking into account the precision of the fused data. An example of data fusion is described in section 4.3.

4. VALIDATION OF THE TECHNIQUES

In the last three years the authors were involved in a European Union Concerted Action called ORFEAS (Optical-Radar Sensor Fusion for Environmental Applications), joining five research groups (University of

Thessaloniki, ICC - Cartographic Institute of Catalonia, ETH Zurich, Technical University of Graz and Polytechnic of Milan). A comprehensive data set, covering South Catalonia (Spain), has been made available to ORFEAS participants by ICC. The above described procedures were validated using a suited reference DEM (coming from aerial photogrammetry) whose precision is one order of magnitude better than that obtainable by radargrammetry and InSAR DEMs. The covered area (approx. 25 by 35 km) includes the flat plain crossed by the Ebro river and a set of mountain chains (the maximum height difference is about 1150 m). This area includes many portions affected by foreshortening, layover and even shadow.

4.1 Radargrammetry Results

The ORFEAS data set includes four Radarsat images, grouped in an ascending pair (ASC) and a descending one (DESC). Each image was captured in a different satellite configuration. Some GCPs were found on the images and their coordinates measured (see Tab. 1). Besides GCPs, a set of tie points between each image pair was obtained in an automatic manner. Moreover, some tie points were manually measured between the ASC and the DESC pairs in order to obtain a geometrically consistent image set. Some of the GCPs were used as control points (check points). A simultaneous bundle adjustment of both pairs was performed using the remaining GCPs and tie points. After eliminating few erroneous points, the refined model parameters were obtained, achieving RMS errors (in the image space) over the check points of 1.54 and 1.35 pixels in azimuth and in range respectively. These values confirm the effectiveness of the model parameter refinement to get an accurate global positioning of the generated grid.

Two DEMs (ASC and DESC) with mesh size of 90 m were generated. The quite large mesh size reflects the poor spatial resolution of the matched points (approx. 1 point per 100 by 100 m). The DEMs were compared with the reference one considering three types of areas: the entire covered area, the flat or hilly portions and the mountainous ones (see Tab. 2). Both ASC and DESC DEMs are unbiased (the global constant bias is 0.08 and 0.11 m respectively), i.e. the generated grids are globally well geo-located. Furthermore, the errors are evenly distributed in the entire scene, i.e. they do not show systematic trends. These characteristics make the data fusion for atmospheric artefact compensation possible.

In Tab. 2, one may notice an important difference in the standard deviations of the hilly/flat and mountainous areas. In the latter ones, the SAR geometric distortions (e.g. foreshortening) are more pronounced and affect the image matching.

Image	Mode	Inclination Angle	# GCPs
ASC_1	SB7	40°.16	12
ASC_2	SB2	24°.46	8
DESC_1	SB1	20°.41	11
DESC_2	SB6	38°.04	16

Table 1: Radarsat images of the ORFEAS data set

The ASC DEM is sensibly better than the DESC one, especially in the mountainous areas. This can partially be explained by the ASC geometric configuration, which has bigger inclination angles and hence is less sensitive to SAR geometric distortions.

The grids coming from the matching of the ASC and DESC pairs were fused in order to estimate a new DEM (named ASC/DESC in Tab. 2). Compared with the previous DEMs, the quality of the new DEM improves sensibly. However, the important difference in the precision over the hilly/flat and mountainous areas (the standard deviation is 21.7 and 30.9 m respectively) still remain.

4.2 InSAR Results

Two ascending ERS-1 images of the ORFEAS data set were chosen for the processing. From the original images two sub-images of 1500 pixels in range by 5000 pixels in azimuth were extracted and processed with the ISAR software. The baseline length is 161.5 m and the mean coherence of the filtered images equals 0.57. The unwrapping generated four major zones of integration. The zones were manually "welded" and the unwrapped phases were checked and corrected for aliasing errors. These operations were very time-consuming (about 12 hours). The InSAR parameters were refined using 14 GCPs. With the unwrapped phases and the refined parameter an irregular grid of 3D points was generated.

DEM type / terrain type	Mean Error [m]	Standard Deviation [m]
ASC – hilly/flat	– 0.23	22.92
ASC – mountainous	0.85	32.84
ASC – entire area	**0.08**	**26.25**
DESC – hilly/flat	0.76	25.54
DESC – mountainous	– 1.49	37.32
DESC – entire area	**0.11**	**29.53**
ASC/DESC – hilly/flat	– 0.39	21.73
ASC/DESC – mountainous	0.01	30.86
ASC/DESC – entire area	**– 0.27**	**24.78**

Table 2: Radargrammetry Results – (90 m mesh size)

DEM type / terrain type	Mean Error [m]	Standard Deviation [m]
Before atmo. correction – hilly/flat	0.25	15.18
Before atmo. correction – mount.	– 4.41	22.71
Before atmo. correction – **entire area**	**– 1.21**	**18.14**
After atmo. correction – hilly/flat	0.29	10.84
After atmo. correction – mountainous	1.08	18.47
After atmo. correction – **entire area**	**0.54**	**13.75**

Table 3: InSAR Results – (30 m mesh size)

The irregular grid of 3D points was interpolated in order to derive a regular one with 30 m spacing. The interpolated grid was compared with the reference DEM (before atmo. correction in Tab. 3). The global (constant) bias of the grid can be considered satisfactory, i.e. the calibration resolves quite well the geo-location of the generated 3D grid. One may notice an important decrease of the DEM precision over mountainous areas (where unwrapping errors occur). The InSAR DEM shows important systematic errors with low spatial frequency characteristics. These errors, due to atmospheric effects, have magnitude up to 30÷35 m. We computed the autocovariance function of the errors: the correlation length is 505 m and the correlation decreases to zero very slowly, i.e. the errors are spatially highly correlated.

4.3 Radargrammetry and InSAR Data Fusion

It is interesting to assess the potential precision of the interferometric DEM not affected by atmospheric distortions. To this purpose, we adopted the strategy described in section 3.2. We used as auxiliary data the ASC DEM coming from radargrammetry: it is less precise than the InSAR DEM, it is much less dense, but it is not affected by systematic errors. From the irregular ASC grid, a 250 m spacing grid was interpolated and fused with the InSAR one, obtaining a new DEM (after atmo. correction in Tab. 3). Most of the systematic effects on the InSAR DEM were removed through the data fusion (except for the mountainous areas where the radargrammetry DEM has bigger errors). One may notice an important improvement of the DEM precision. The correlation length of the errors is 105 m, which confirms the effectiveness of the artefact correction. In fact, the errors of the new DEM are almost spatially decorrelated because the systematic errors caused by atmospheric heterogeneity were properly removed.

5. CONCLUSIONS

Two new procedures (radargrammetric and InSAR approaches) for DEM generation have been described. Their most original parts are the rigorous geometric models used in the DEM generation and the refinement of the model parameters (calibration). The procedures were validated employing a suite reference one. Over the considered test area, radargrammetry generated in a fully automatic way DEMs with a quite good global accuracy. However, an important degradation of the DEM quality in mountain areas occurred. Compared with InSAR, radargrammetry DEMs have poorer resolution, are less precise but their quality is independent of atmospheric conditions during image acquisition. InSAR DEMs have high spatial resolution and good precision over hilly/flat terrain. Their precision is quite degraded in mountain areas and can be affected by atmospheric artefacts. A strategy to reduce such artefacts using auxiliary low-resolution data has been proposed. Employing a radargrammetry grid as auxiliary data, the data fusion increased considerably the InSAR DEM precision.

ACKNOLEDGEMENTS

The authors thank Dr. Paolo Pasquali (now at RSL, University of Zurich) and Prof. Claudio Prati (from DEI, Polytechnic of Milan) for kindly providing the software for phase unwrapping.

REFERENCES

[1] B. Mercer, et al, “Relief restitution by radar-grammetry”. Proc. of the Second ERS Applications Workshop, London, 6-8 December, pp. 277-281, 1986.

[2] T. Toutin, “Generating DEM from stereo images with a photogrammetric approach: Examples with VIR and SAR data”. EARSeL Journal Advances in Remote Sensing, vol. 4, no. 2, pp. 110-117, 1995.

[3] H. Ramapryiyan, “Automated matching of pairs of SIR-B images for elevation mapping”. IEEE Transaction on Geosciences and Remote Sensing, vol. 24, no. 4, pp. 462-471, 1986.

[4] L. Marinelli and L. Laurore, “Relief restitution by radargrammetry”. Proc. of 2nd ERS Applications Workshop, London, pp. 277-281, 1996.

[5] H.A. Zebker and R.M. Goldstein, “Topographic Mapping from Interferometric SAR Observations”. Journal of Geophysical Research, Vol. 91, No. B5, pp.4993-4999,1986.

[6] W. Förstner, E. Gülch, “A fast operator for detection and precise location of distinct points, corners and centers of circular features”. Proceedings of the Conference on Fast Processing of Photogrammetric Data, Interlaken (CH), pp. 281-305, 1987.

[7] J. Koskinen, “The ISAR-Interferogram Generator Manual”. ESA/ESRIN, Frascati, Italy, 1995.

[8] R.M. Goldstein and H.A. Zebker, “Two-dimensional Phase Unwrapping”. Radio Science, Vol. 23, No. 4, pp.713-720, 1988.

[9] R. Hanssen, “Atmospheric heterogeneities in ERS tandem SAR interferometry”. DEOS Report, No. 98.1, Delft University Press, Delft, 1998.